Surface magnetism in ZnO/Co_3O_4 mixtures

M. A. García,[1,2,a)] F. Jiménez-Villacorta,[3] A. Quesada,[4] J. de la Venta,[1,2] N. Carmona,[2] I. Lorite,[1] J. Llopis,[2] and J. F. Fernández[1]
[1]*Instituto de Cerámica y Vidrio, Consejo Superior de Investigaciones Científicas, 28049 Madrid, Spain*
[2]*Dpto. Física de Materiales, Universidad Complutense de Madrid, 28040 Madrid, Spain*
[3]*SpLine, Spanish CRG Beamline, ESRF F-38043 Grenoble, Cedex 09 France and Instituto de Ciencia de Materiales de Madrid, Consejo Superior de Investigaciones Científicas, 28049 Madrid, Spain*
[4]*Lawrence Berkeley National Laboratory, Berkeley, California 94720, USA*

(Received 6 October 2009; accepted 18 December 2009; published online 23 February 2010)

We recently reported the observation of room temperature ferromagnetism in mixtures of ZnO and Co_3O_4 despite the diamagnetic and antiferromagnetic character of these oxides, respectively. Here, we present a detailed study on the electronic structure of this material in order to account for the unexpected ferromagnetism. Electrostatic interactions between both oxides lead to a dispersion of Co_3O_4 particles over the surface of ZnO larger ones. As a consequence, the reduction $Co^{+3} \rightarrow Co^{2+}$ at the particle surface takes place as evidenced by x-ray absorption spectroscopy measurements and optical spectroscopy. This reduction allows explaining the observed ferromagnetic signal within the well established theories of magnetism in oxides. © *2010 American Institute of Physics*. [doi:10.1063/1.3294649]

I. INTRODUCTION

In the past years, a large number of reports have shown unexpected ferromagnetism (FM) in oxides, mainly in thin films and nanostructured materials (for a general review, see Ref. 1). These effects have been ascribed to diluted magnetic semiconductor oxides (DMSO),[2–4] doping induced,[5–7] nanoscale, surface,[8] and proximity effects.[9] However, there is still a large controversy about these new results including possible experimental errors,[10] and the origins of this phenomenology are not clear at all. We recently reported room temperature (RT) FM in mixtures of ZnO and Co_3O_4 despite the diamagnetic and antiferromagnetic character of both oxides, respectively.[11] As Fig. 1 summarizes, the FM appears after soft milling of the mixed oxides and decreases after annealing, disappearing for thermal treatments over 700 °C. Therefore, the effect arises when surfaces of both oxides come in contact interacting weakly and disappears as they react to form a complex oxide (discarding the possibility to have a DMSO). At that time we could not propose an explanation for the appearance of the RT FM but just indicate that the effect exists, it was not a measuring artifact nor due to metallic Co segregation or sample contamination. We present here a study on the electronic structure of the ZnO/Co_3O_4 mixtures in order to understand the origin of this surprising effect. We show that the presence of a RT FM signal is due to a surface effect that can be explained with the well known theories of the magnetism of oxides.

II. EXPERIMENTAL

$ZnO_{1-x}(Co_3O_4)_x$ samples with x=0.01, 0.05, and 0.25 were prepared as already described in Ref. 11. Briefly, powders were attrition milled in water medium with zirconia balls, dried, sieved, and prereacted afterwards at 400 °C for 8 h separately in an alumina crucible. Calcined powders were mixed and attrition milled again. The dried and sieved powders pressed into disks (20 mm in diameter and 2 mm in thickness) were annealed at different temperatures ranging from 500 to 1000 °C in air. Two set of samples were prepared from high purity raw powders independently in two different laboratories (affiliations 1 and 2) and using materials from different suppliers.

The structural analysis of the samples was carried out with a Siemens D5000 x-ray diffractometer using a monochromatic Cu K line and operating at 40 kV and 40 mA. The microstructure of the samples was observed with a field emission scanning electron microscope (FE-SEM) (Hitachi S-4700, Japan) coupled with an energy dispersed spectroscopy system. Magnetic characterization was performed in two different vibrating sample magnetometers (VSMs), a VSM LDJ Instruments and a VSM Lakeshore 7304. For the magnetic measurements, all possible sources of experimental errors described in Ref. 10 were taken into account. Optical absorption was measured with a Shimadzu 3101 spectrophotometer attached with an integrating sphere. X-ray absorption near edge spectroscopy (XANES) measurements at the Co K-edge energies were performed in the transmission

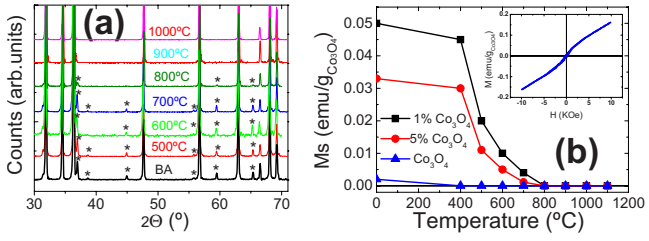

FIG. 1. (Color online) (a) XRD patterns from the samples with 95% ZnO–5% Co_3O_4. Asterisks indicate Co_3O_4 peaks while nonindexed peaks correspond to ZnO. BA stands for before annealing. (b) Saturation magnetization as a function of the annealing temperature. Inset shows the magnetization curve at 300 K for the sample with 5% Co_3O_4 after milling.

a)Electronic mail: magarcia@icv.csic.es.

mode at the Spanish CRG beamline (SpLine), at the ESRF. Two gas ionization chambers, filled with nitrogen and argon, were used to measure the incident and the transmitted beam, respectively. Several scans were taken, in order to obtain a good signal-to-noise ratio.

We will focus here on the samples consisting on 5% Co_3O_4–95% ZnO. For the samples with 1% Co_3O_4, the x-ray absorption spectroscopy (XAS) and magnetic measurements were noisy and close to the resolution limit of the equipment (although magnetic measurements showed the highest values when normalized to the Co_3O_4 content). On the contrary, for the samples with 25% of Co_3O_4 the effect is quite reduced, probably because a smaller fraction of Co_3O_4 is in contact with ZnO.

III. RESULTS AND DISCUSSION

Figure 1 summarizes the x-ray diffraction (XRD) and magnetic measurements already reported.[11] Briefly, the XRD patterns [Fig. 1(a)] show just the peaks corresponding to ZnO and Co_3O_4 for the samples milled and annealed up to 1000 °C. Diffractograms of the samples milled and annealed at 500 and 600 °C result equivalent, indicating the presence of both oxides; annealing at higher temperatures yield a decrease in the Co_3O_4 peaks without any other new peaks appearing in the diffraction pattern. This result indicates that there is no significant diffusion up to 600 °C while at larger temperatures the Co diffuses into ZnO to form a $Zn_{1-x}Co_xO$ solid solution, isostructural with the ZnO (and therefore explaining the absence of new peaks in the XRD patterns).

Samples exhibited paramagnetic behavior at RT with a superimposed ferromagnetic contribution that disappears after annealing at 700 °C [Fig. 1(b)]. The magnetic effects were found to be reproducible for both sets of samples (i.e., the observation of RT ferromagnetic component for samples annealed up to 600 °C), but changes in the magnetization values up to 35% were found between both sets. Figure 1(b) shows the data for the set exhibiting the largest M_S values).

A. SEM analysis

Figure 2 shows a FE-SEM image of a sample consisting on 5% Co_3O_4–95% ZnO softly milled. After milling, Co_3O_4 particles resulted deagglomerated and dispersed over the surface of large ZnO particles. This dispersion is the fingerprint of a strong interaction between both oxides; the reason for this effect is related to the differences of surface charge between ZnO and Co_3O_4 that promotes the dispersion of Co_3O_4 onto ZnO large particles driven by electrostatic forces.[12,13]

FIG. 2. FE-SEM micrograph for the 5% Co_3O_4–95% ZnO sample after milling showing the Co_3O_4 particles dispersed over the surface of large ZnO ones.

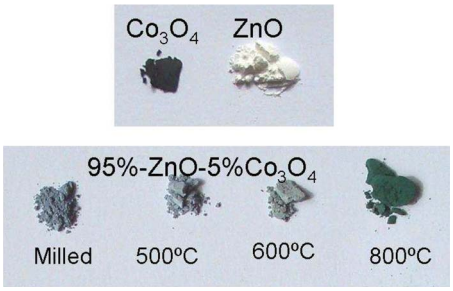

FIG. 3. (Color online) Pictures of (top) ZnO and Co_3O_4 powder and (bottom) mixtures 5% Co_3O_4–95% ZnO after milling and annealing at different temperatures.

B. Optical absorption

Figure 3 shows pictures of the samples were clear differences in color are observed. While ZnO and Co_3O_4 exhibit white and black color, respectively, milled samples and those annealed at 500 and 600 °C resulted blue (a color that cannot be achieved by combination of black and white), confirming that there is a modification of the electronic structure just after mixing. The sample annealed at 800 °C results greenish which is the characteristic color of $ZnCo_2O_4$, in agreement with the XRD data.

A more detailed analysis of these visual changes can be performed by means of optical spectroscopy. Figure 4(a) displays the optical reflectance spectra in the UV-visible part of the spectrum. Pure ZnO spectrum exhibits the characteristic shape for semiconductors with a flat plateau over the band-gap (around 400 nm) and a sharp decrease at the edge, while Co_3O_4 spectrum shows a "surfing profile" with very low reflectance values. The samples containing 5% Co_3O_4 just milled and those annealed at 500 and 600 °C (i.e., the magnetic samples) showed a nonflat profile spectrum with a maximum of the reflectance at 400 nm associated with the samples blue color. This maximum is due to the combination of the ZnO band edge at lower wavelengths and a broad absorption band in the visible part of the spectrum. The sample annealed at 800 °C shown a complete different spectrum with strongly reduced reflectance and a maximum at about 500 nm responsible for the green color.

Figure 4(b) presents the spectrum obtained by linear combination of 5% of Co_3O_4 and 95% of ZnO and that corresponding to the milled sample. The evident differences between both spectra, confirm the reaction between ZnO and Co_3O_4 after milling, leading to a modification of the electronic structure that is the ultimate responsible of the material optical properties. This modification of the electronic configuration of ZnO (and consequently on that of Co_3O_4) just after milling seems to be in the origin of the observed

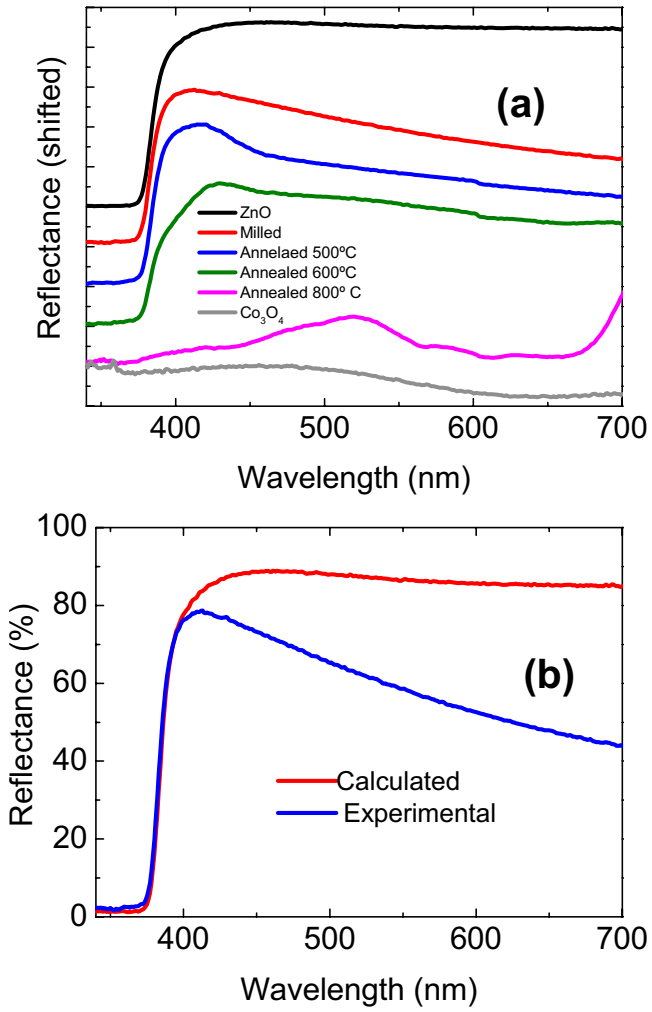

FIG. 4. (Color online) (a) Diffused reflectance spectra of the samples (curves are shifted vertically for clarity). (b) Spectra for 5% Co_3O_4–95% ZnO experimentally measured for the milled samples and that calculated by linear combination of ZnO (95%) and Co_3O_4 (5%) spectra.

FM. Actually, the three samples exhibiting RT FM show a very similar reflectance spectra profile, supporting this hypothesis.

Deep blue color is characteristic of compounds containing Co^{+2} in tetrahedral positions that arise two absorption peaks centered at 435 and 729 nm.[14] These peaks correspond to the ligand to metal $[p(O^{2-}) \rightarrow e_g(Co^{3+})]$ and metal to metal $[t_{2g}(Co^{3+}) \rightarrow t_2(Co^{2+})]$ charge transfer, respectively. However, the light blue coloration in our samples is fairly different to that characteristic of materials containing tetrahedral Co^{2+} (that tends to be darker). Actually, we just find a very broad absorption band in the reflectance spectrum (Fig. 4) in contrast with the two bands indicated above.

A broad absorption band in the visible part of the spectrum and blue coloration similar to that reported here have been ascribed to the coexistence on Co^{2+} in both tetrahedral and octahedral positions in different matrices.[15,16] Co^{2+} in octahedral positions generates absorption bands that overlaps those of the tetrahedral Co, yielding to a broad absorption spectrum.[17] For Co_3O_4, tetrahedral positions are occupied by Co^{+2} while Co^{+3} are placed in octahedral ones.[18] Thus, there

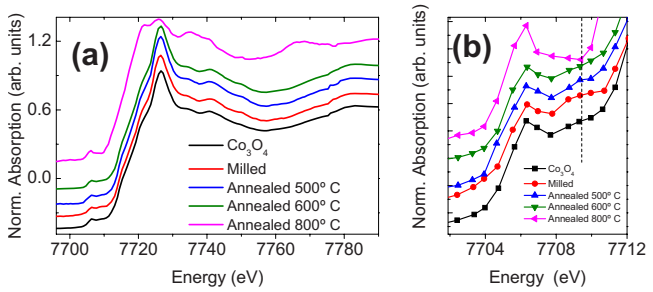

FIG. 5. (Color online) (a) XANES Co K-edge spectra of the samples; a pure Co_3O_4 XANES has been added as reference; (b) detail of the XANES spectra at the pre-edge region. (Curves are shifted vertically for clarity.)

are no Co^{+2} ions in octahedral positions. However, if Co^{+3} ions in octahedral position are reduced to Co^{+2} without any modification of the crystallographic structure, the light blue color and a broad absorption band could be explained. Such a reduction could be promoted by the interaction of ZnO considering the strong electrostatic interaction between both oxides.[12,13] During the milling process, some Co^{+2} in the surface of Co_3O_4 could be reduced keeping the crystal structure (as evidenced by XRD). This region should be small and close to the surface. A massive reduction of Co^{+3} to Co^{+2} will render the crystallographic structure unstable and the oxide will transform into CoO. The absence of changes in the XRD patterns after mixing indicates that any modification due to the interaction between both oxides is limited to the surface region where both oxides are in contact. However, there are many defects in ZnO that could also account for the observed blue color.[19] In order to elucidate the possible reduction in Co ions we used an element specific technique as XAS.

C. X-ray absorption spectra

The x-ray absorption spectra measured at the Co K-edge are presented in Fig. 5(a). The spectra for the samples with 5% Co_3O_4 milled and annealed up to 600 °C are very similar to that of pure Co_3O_4 in agreement with the XRD presented on Fig. 1. For the sample annealed at 800 °C the spectrum is fairly different, due to the already mentioned formation of $ZnCo_2O_4$. Although standard XANES is a bulk spectroscopy, the resulting spectrum comes from the weighted contribution of every Co atom in the sample. In the case of nanoparticle systems, an enhanced contribution of atoms located at the surface is expected, rending XANES sensitive to surface modifications.[20] These spectra show a pre-edge feature [Fig. 5(b)] with a maximum at about 7707 eV. This maximum corresponds to a forbidden quadrupolar transition $1s \rightarrow 3d$, in which the 3d level presents a *p* character due to *pd* hybridization. However, after milling, a second weak peak appears at energies slightly larger than the main peak (around 7710 eV); this second peak is present for milled samples and those annealed at 500 °C while it cannot be observed for larger annealing temperatures (i.e., it is present in the samples exhibiting magnetic behavior). This result suggests a slight modification in the electronic structure of Co atoms after milling, which may be in the origin of

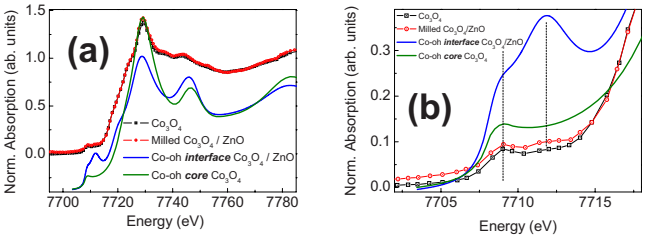

FIG. 6. (Color online) (a) Calculations of the contribution to the XANES of absorbing Co octahedral atoms located at the core of the Co_3O_4 particle (green) and the Co_3O_4/ZnO interface (blue), compared with the milled sample and the Co_3O_4 reference; (b) detail of the calculated and experimental XANES spectra at the pre-edge region.

the observed FM. In order to understand these modifications, a qualitative study by means of XANES calculations was carried out.

XANES calculations have been performed within the real-space multiple-scattering formalism of the FEFF8 code. Self-consistent computations were achieved choosing a cluster of around 4 Å. Spherical atomic potentials have been proposed using the muffin-tin approximation, with default overlapping of spherical potentials of 15%. Several exchange and correlation potentials have been tested. A complex Dirac–Hara (DH) electronic potential, in which we add the Hedin–Lundqvist imaginary part to the classical DH expression is found to perform a better reproducibility of both the position and the intensity of the experimental features. No extra broadening has been applied in the computations. Two clusters have been used to account for two different contributions according to the local structure around Co atoms: absorbing Co atom in octahedral position in a Co_3O_4 cluster (Co-oh core) and absorbing Co atom in octahedral position located at the interface between the Co_3O_4 and the ZnO (Co-oh interface).

Results of the calculations are shown in the Fig. 6. The calculated XANES spectra accounting for the two different environments (core and interface) show similarities in the position and the intensity of features located in the namely XANES region, above the white line. Visible differences are observed in the edge region. In the Co-oh interface calculated spectrum, the pre-edge region shows a double structure. The two pre-edge peaks appearing in the Co-oh interface cluster calculation evidence that the secondary feature appearing in the FM samples comes from the contribution of Co atoms at the interface [Fig. 5(b)]. Furthermore, the secondary feature presents a remarkable intensity, in such a manner that even a very small contribution coming from the Co-oh interface atoms will lead to a small but visible, enhancement in such feature in the experimental XANES spectrum. Moreover, the edge of the Co-oh interface XANES is found to be slightly shifted ($\approx$2 eV) to lower energies, respect to the Co-oh core one. This feature, in agreement also with the decrease in intensity in the white line in the interface contribution, suggests a decrease in the oxidation state of the octahedral Co atoms at the surface, which supports the idea of the reduction $Co^{3+} \rightarrow Co^{2+}$ in the octahedral Co atoms located at the interface regions.

While we could not perform a definitive experiment to confirm the surface reduction of Co_3O_4, it is worthy to note that this hypothesis allows explaining simultaneously the changes in the XAS spectra, optical spectra, and magnetization curves. Thus, although not fully proven, the reduction of Co^{+3} is strongly supported by the combination of experimental results. XAS spectra confirm the modification of the Co_3O_4 electronic structure; moreover the observation of magnetic features also points on this direction considering that ZnO is diamagnetic. The reduction in the Co^{+3} lead to an optical spectra (Fig. 4) very similar to those already published[15,16] when a combination of Co^{+2} in both tetrahedral and octahedral position are presented (a situation that can be achieved in Co_3O_4 by Co^{+3} reduction); the shape of the experimental XANES pre-edge also fits the spectrum calculated for Co_3O_4 assuming a reduction of Co^{+3}.

A modification of the Co_3O_4 structure at the surface could also account for the observed modification but is not likely because of several reasons. First, the soft milling performed to mix both oxides is not expected to induce structural changes and no modifications were found in the XRD patterns. Actually, after milling and annealing no structural changes are found up to annealing temperatures of 700 °C so it is rather unlikely that a structural change takes place during milling (note that no change in the particle size was found after milling according to SEM observations). The pure Co_3O_4 milled in the same conditions showed no changes either in the optical and XAS spectra nor in the magnetization curves; thus we can rule out a modification of the structure due to the mechanical milling process. Therefore, the reduction $Co^{+3} \rightarrow Co^{+2}$ results likely and allows to explain the changes observed in the XAS and optical spectra (and as explained below, also in the magnetic properties).

The phenomenology described here, is fairly similar to that observed in mixtures of anatase TiO_2–Co_3O_4 and can be interpreted in the same way.[21] Co_3O_4 possess the same spinel structure that Fe_3O_4, with Co^{+2} in tetrahedral positions and Co^{+3} in octahedral ones. In this kind of spinels, antiferromagnetic interactions between octahedral and tetrahedral cations are the dominant ones[18] leading to the well known ferrimagnetic character of ferrites (due to the different number of sites and magnetic moment of octahedral and tetrahedral positions) with high Curie Temperature (T_C); e.g., 858 K for Fe_3O_4 or 673 K for $NiCo_2O_4$. As Fig. 7 illustrates, the magnetic moment of Co ions depends on the oxidizing state and also on the symmetry of the crystal field, which determines the splitting of the doublet t_{2g} and triplet e_g states. For Co_3O_4, the Co^{+2} ions in tetrahedral position hold no magnetic moments.[18] Thus, there are no antiferromagnetic interactions between tetrahedral and octahedral Co ions. In this situation, the weaker antiferromagnetic interaction between Co^{+3} in octahedral positions becomes the dominant one, arising then the well known antiferromagnetic character of this oxide with low Neel temperature (40 K).

If we assume that the reduction process suggested by XAS and optical experiments takes place without structural modifications, there will be regions of the crystal close to the surface where Co^{+3} is reduced to Co^{+2}. In this regions there will be Co ions holding a magnetic moment in both tetrahe-

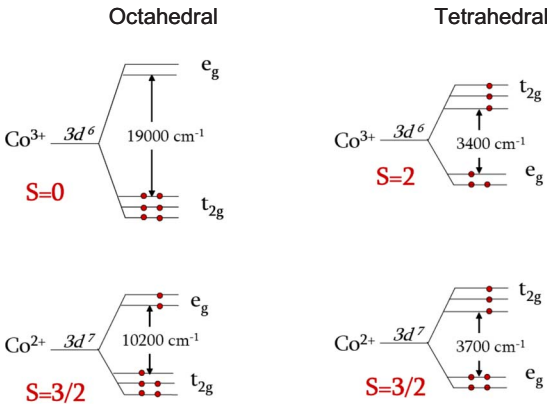

FIG. 7. (Color online) 3d band splitting for Co^{+2} and Co^{+3} ions in presence of an octahedral and tetrahedral crystal field.

dral and octahedral positions. Then, the leading magnetic interaction will be antiferromagnetic between octahedral and tetrahedral positions. The situation will be very similar to that of Fe_3O_4 and the expected magnetic behavior should be the same: ferrimagnetism with high T_C. Thus, we should expect a mixture of paramagnetism (from the grains core that remains unaffected) and a small ferrimagnetic signal coming from the reduced surface regions. In this way, it is possible to explain the presence of RT FM in the ZnO/Co_3O_4 mixtures based on the well established theories of magnetism in oxides and no new magnetic order mechanism are required to account for the observed FM.

IV. CONCLUSIONS

In summary, we demonstrated here that mixing and soft milling of ZnO and Co_3O_4 lead to a dispersion of the Co_3O_4 particles on the surface of large ZnO ones. Optical spectroscopy and XAS measurements strongly suggest that this interaction causes a surface reduction of Co^{+3} in octahedral positions to Co^{+2}. In the Co_3O_4 surface where this reduction takes place, the structure and electronic configuration should be similar to that for Fe_3O_4, explaining the observation ferromagnetic features (actually ferrimagnetic) in the magnetization curves with the superexchange interactions of oxides.

ACKNOWLEDGMENTS

Lucas Perez and Manuel Plaza are acknowledged for the help with the magnetic measurements. M.S. Martín-González and J. L. Costa-Krämer are acknowledged for fruitful discussions. This work was supported by the Spanish Council for Scientific Research through Project Nos. CSIC 2006-50F0122 and CSIC 2007-50I015 and Spanish Ministry of Science and Education through Project Nos. MAT2007-66845-C02-01 and FIS-2008-06249. We acknowledge the European Synchrotron Radiation Facility for provision of synchrotron radiation facilities and we would like to thank the SpLine CRG beamline staff for assistance during x-ray absorption experiments.

[1] J. M. D. Coey and S. A. Chambers, MRS Bull. **33**, 1053 (2008).
[2] Y. Matsumoto, M. Murakami, T. Shono, T. Hasegawa, T. Fukumura, M. Kawasaki, P. Ahmet, T. Chikyow, S. Koshihara, and H. Koinuma, Science **291**, 854 (2001).
[3] P. Sharma, A. Gupta, K. V. Rao, F. J. Owens, R. Sharma, R. Ahuja, J. M. Osorio Guillén, B. Johansson, and G. A. Gehring, Nature Mater. **2**, 673 (2003)
[4] J. M. D. Coey, Curr. Opin. Solid State Mater. Sci. **10**, 83 (2006).
[5] K. R. Kittilstved and D. R. Gamelin, J. Am. Chem. Soc. **127**, 5292 (2005).
[6] K. R. Kittilstved, N. S. Norberg, and D. R. Gamelin, Phys. Rev. Lett. **94**, 147209 (2005).
[7] D. Rubi, J. Fontcuberta, A. Calleja, Ll. Aragonès, X. G. Capdevila, and M. Segarra, Phys. Rev. B **75**, 155322 (2007).
[8] M. Venkatesan, C. B. Fitzgerald, J. M. D. Coey, Nature (London) **430**, 630 (2004).
[9] A. Brinkman, M. Huijben, M. van Zalk, J. Huijben, U. Zeitler, J. C. Maan, W. G. van der Wiel, G. Rijnders, D. H. A. Blank, and H. Hilgenkamp, Nature Mater. **6**, 493 (2007).
[10] M. A. García, E. Fernández Pinel, J. de la Venta, A. Quesada, V. Bouzas, J. F. Fernández, J. J. Romero, M. S. Martín-González, and J. L. Costa-Krämer, J. Appl. Phys. **105**, 013925 (2009).
[11] A. Quesada, M. A. García, M. Andrés, A. Hernando, J. F. Fernández, A. C. Caballero, M. S. Martín-González, and F. Briones, J. Appl. Phys. **100**, 113909 (2006).
[12] M. S. Martín-González, M. A. García, I. Lorite, J. L. Costa-Krämer, F. Rubio-Marcos, N. Carmona, and J. F. Fernández, J. Electrochem. Soc. **157**, E31 (2010).
[13] I. Lorite *et al.* (unpublished).
[14] S. Thota, A. Kumar, and J. Kumar, Mater. Sci. Eng., B **164**, 30 (2009).
[15] P. Lommens, F. Loncke, P. F. Smet, F. Callens, D. Poelman, H. Vrielinck, and Z. Hens, Chem. Mater. **19**, 5576 (2007).
[16] M. Zayat and D. Levy, Chem. Mater. **12**, 2763 (2000).
[17] G. Y. Lee, K. H. Ryu, H. G. Kim, and Y. Y. Kim, Bull. Korean Chem. Soc. **30**, 373 (2009).
[18] W. L. Roth, J. Phys. Chem. Solids **25**, 1 (1964).
[19] C. Klingshirn, R. Hauschild, H. Priller, M. Decker, J. Zeller, and H. Kalt, Superlattices Microstruct. **38**(4-6), 209 (2005).
[20] P. Zhang and T. K. Sham, Appl. Phys. Lett. **81**, 736 (2002).
[21] A. Serrano, E. Fernández Pinel, A. Quesada, I. Lorite, M. Plaza, L. Pérez, F. Jiménez-Villacorta, J. de la Venta, M. S. Martín-González, J. L. Costa-Krämer, J. F. Fernández, J. Llopis, and M. A. García, Phys. Rev. B **79**, 144405 (2009).